Received: 31 July 2018 | Revised: 28 February 2019 | Accepted: 26 March 2019

DOI: 10.1002/ett.3620

RESEARCH ARTICLE

WILEY

Extended reduced-rank joint estimation of direction of arrival with mutual coupling for coherent signals

Nann Win Moe Thet[1] | Amit Kachroo[2] | Mehmet Kemal Ozdemir[3]

[1]Graduate School of Engineering and Natural Sciences, Istanbul Medipol University, Istanbul, Turkey

[2]Department of Electronics and Computer Engineering, Istanbul Sehir University, Istanbul, Turkey

[3]School of Engineering and Natural Sciences, Istanbul Medipol University, Istanbul, Turkey

Correspondence
Nann Win Moe Thet, Graduate School of Engineering and Natural Sciences, Istanbul Medipol University, 34810, Istanbul, Turkey.
Email: nthet@st.medipol.edu.tr

Present Address
Nann Win Moe Thet, Graduate School of Engineering and Natural Sciences, Istanbul Medipol University, 34810, Istanbul, Turkey

Funding information
TÜBİTAK, Grant/Award Number: 215E316; TÜBİTAK 2215 BİDEB Scholarship Program

Abstract

This paper proposes an extended method for direction-of-arrival (DOA) estimation with unknown mutual coupling for coherent signals. The proposed method employs the forward/backward spatial smoothing to decorrelate the coherent signals in the process of rank reduction with the joint iterative subspace optimization approach. Then, the autocalibration of mutual coupling is performed based on the Capon's minimum variance criterion. Performance of the proposed method is compared with the state of the art algorithms in terms of DOA root-mean-square error and in terms of probability of successful estimation, where successful estimation is the case when the average of absolute DOA estimation error is within 2.5°. It is shown that the proposed method has a similar performance as the state of the art autocalibration methods while offering a lower computational complexity.

1 | INTRODUCTION

Direction-of-arrival (DOA) estimation of multiple narrowband signals has been extensively studied in the field of radar and sonar communications for civilian and military purposes. In recent years, the attention has been extended into cellular systems such as current fourth generation (4G)/ long-term evolution (LTE) communications and millimeter wave (mmWave) communications for future fifth generation (5G) and beyond technologies. In these systems, advanced beamforming techniques are employed at the base stations (BSs) in order to provide services to many users simultaneously.[1-3] With the knowledge of direction of the incoming signals, BSs perform adaptive beamforming by steering transmitted beams toward desired users while minimizing the undesired users' interference. Overall, systems with much higher capacity than the existing systems are anticipated.

For 5G and beyond systems, multiple antennas in the order of hundreds are proposed in order to compensate for the path loss of high frequency carriers. This technique is termed as massive multiple-input–multiple-output (MIMO).[4,5] The use of many closely packed antennas, however, introduces mutual coupling (MC) between the antenna elements.[6,7] With multiple directional beams targeting different user groups in massive MIMO 5G systems, accurate estimation of DOA

 © 2019 John Wiley & Sons, Ltd.

of the incoming signals becomes an important task especially in the presence of MC, as a small DOA estimation error decreases, the signal-to-interference-plus-noise ratio and thereby reduces the system capacity.[8]

1.1 | Related work

Many high-resolution techniques have been proposed in the literature over the past decades. Among them, the most popular techniques are the Capon algorithm[9] and the subspace-based approaches such as *Estimation of Signal Parameters via Rotational Invariance Techniques* (ESPRIT)[10,11] and *MUltiple SIgnal Classification* (MUSIC).[12,13] While Capon algorithm suffers from computationally heavy matrix inversion, ESPRIT and MUSIC algorithms suffer from high complexity due to singular value decomposition or eigenvalue decomposition (EVD). As a way of reducing the computational complexity, reduced-rank approaches have been developed.[14,15]

Most of the high-resolution methods consider the signals to be noncoherent and the array manifold to be perfectly known. However, wireless channels include multipath propagation, resulting in highly correlated or coherent signals, which then cause the high resolution of DOA estimation techniques to degrade.[16-18] This is a major problem for the upcoming 5G systems, where massive MIMO systems are to be deployed for spatial multiplexing. Moreover, the array manifold is usually affected by MC of the array elements, which adversely affects the estimation accuracy.[19]

The algorithms that have been proposed to improve the DOA estimation performance in the presence of unknown MC typically exploit autocalibration technique.[20-23] This approach has the ability to estimate DOA and MC jointly without any calibration sources. For 2-dimensional (2D) DOA estimation with MC in a uniform circular array, Jiang et al[24] proposed an algorithm that iteratively modifies the beamspace data. In the work of Wu et al,[25] a subspace-based rank-reduction method is proposed for a uniform rectangular array. However, these methods assume that the signals are uncorrelated. Besides, the iterative calibration process in some of these methods[23,24] results in a higher computational complexity for massive MIMO systems.

To tackle the issue of coherent signals, various approaches have been considered. However, the spatial smoothing (SS) approach particularly has received more attention.[16-18] Moreover, without considering MC in the system, orthogonal projection methods that are based on array steering matrix[26] and signal subspace[27] have also been proposed to estimate the DOA of the coherent signals in low-altitude environments. Especially, in the work of Zhou et al,[27] SS method is incorporated to decorrelate the received signals with lower computational complexity. However, as the number of array elements and the sample size increase, the complexity gets higher. With unknown MC, DOA of coherent signals is estimated by using a conventional subspace-based method in conjunction with the SS scheme.[28,29] In the works of Dai and Ye[28] and Liao and Chan,[29] algorithms with the SS technique for the estimation of DOAs of the coherent signals without finding the MC estimates are proposed. However, these approaches suffer from the loss of array aperture since they only utilize the middle subarrays. Thus, these methods are not practical for antenna arrays with large number of elements.

Shi et al[30] proposed another 2D DOA estimation algorithm for coherent signals, where the algorithm utilizes the received signal obtained from the whole two parallel uniform linear array (ULA) elements in order to reconstruct two new Toeplitz matrices based on fourth-order cumulants. By using the new Toeplitz matrices,[30] the algorithm decorrelates the signals effectively while avoiding the loss of array aperture. In another study, to decorrelate the coherent signals for correct DOA estimation, Shi et al[31] proposed an improved spatial differencing (ISD), where difference-operation is performed only on autocorrelations of the subarray outputs instead of the whole correlations, along with forward only ISD and backward only ISD. The study can be seen as an extended work of Qi et al.[32] With the improved ISD, the estimation performance is comparatively better than the conventional SS approaches as the effect of additive white or colored noise in the problem is suppressed more effectively. However, this algorithm does not consider the MC effect of the array and it is also difficult to adapt the algorithm for coupling autocalibration techniques.

1.2 | Motivation

Reviewing the works of Toşa[1] and Qi et al,[32] we observe that there is still a need to develop an algorithm that can jointly estimate the DOA and MC of coherent signals while providing a lower computational cost. In our previous works,[33,34] we proposed a reduced-rank–based algorithm for joint estimation of DOAs and MC, where a new reduced-rank covariance matrix of the array output obtained from reduced-rank joint iterative subspace optimization (JIO) algorithm[14] was employed to jointly estimate DOAs and MC by using the iterative autocalibration approach.[23] However, in those works, the signals were assumed to be uncorrelated. Therefore, a low complexity joint estimation of DOAs and MC in the presence of

coherent signals needs to be further investigated. Hence, this paper focuses on an improved low complexity algorithm for estimating DOAs of the coherent signals with MC by utilizing the forward/backward SS (FBSS) preprocessing scheme.[16,17] The main difference between the current work and the previous work is that JIO algorithm is modified and integrated with the FBSS process in the presence of MC, which is named as FBSS-JIO, and after estimating the MC coefficients from autocalibration algorithm, an additional FBSS-JIO is performed with the newly estimated MC coefficients in order to obtain more accurate DOA estimates.

1.3 | Contributions and paper organization

As discussed in Section 1.1, there is an ongoing research about the analysis of the reduced-rank–based DOA estimation with MC or without MC and the DOA estimation of coherent signal with MC or without MC. However, joint estimation of DOA and MC for coherent signals that provides low computational cost still needs further investigation. Therefore, in this paper, we propose a low computational complexity DOA estimation of coherent signals in the presence of MC. For the proposed method, the reduced-rank–based DOA estimation with unknown MC that was studied in our previous works[33,34] is modified and extended for the case of coherent signals.

Firstly, in Section 2, we describe the system model for ULA and briefly introduce the FBSS method. Then, the proposed algorithm for joint estimation of DOAs and MC for the coherent signal is explained in Section 3. In order to decorrelate the coherent signals in the presence of MC, in Section 3.1, we made a modification to the conventional FBSS preprocessing scheme by including the MC matrix (MCM), which has the same size as the subarray size in FBSS process. Then, in Section 3.2, the rest of the proposed algorithm is presented as follows. First, JIO-FBSS–based reduced-rank DOA estimation problem with MC is reformulated by applying the newly modified FBSS in the reduced-rank JIO algorithm, which is further revised to adapt the FBSS. Then, the modified coupling autocalibration[23,34] is performed to iteratively update the coupling.

After the MC coefficients are estimated, unlike the previous work,[34] DOA estimates are obtained from FBSS-based JIO method using the estimated MC coefficients. In contrast to our previous approach,[33] where the existing subspace-based autocalibration method[23,35] is employed, in the current work, the autocalibration is based on the minimum variance (MV) criterion. To the best of our knowledge, only our current work considers the reduced-rank JIO algorithm in the matter of joint estimation of DOAs and MC of the coherent signals.

In summary, our main contributions over the existing algorithms and our previous work are (a) to reformulate the JIO-FBSS algorithm suitable for MC autocalibration and (b) to exploit a new reduced-rank spatially smoothed covariance matrix in the MV-based joint estimation of DOAs and MC while maintaining low complexity. The performance analysis in terms of root-mean-square error (RMSE) and success probability is presented in Section 4. Finally, Section 5 concludes this paper.

2 | SYSTEM MODEL

For the system model, we assume that M narrowband signals $\{s_m\}_{m=1}^{M}$ arrive from different angles $\{\theta_m\}_{m=1}^{M}$ at a ULA with N identical sensors, each equally spaced by d interelement distance, as depicted in Figure 1. Assuming that the steering vectors of the sources are not perfectly known due to MC, the resulting complex vector of the array output $\boldsymbol{x}(k) \in \mathbb{C}^{N\times 1}$ at k^{th} snapshot can be modeled as

$$\boldsymbol{x}(k) = \boldsymbol{CAs}(k) + \boldsymbol{n}(k) \qquad k = 1, 2, \ldots, K, \tag{1}$$

where $\boldsymbol{s}(k) = [s_1(k), \ldots, s_m(k)]^T \in \mathbb{C}^{M\times 1}$ and $\boldsymbol{n}(k) = [n_1(k), \ldots, n_m(k)]^T \in \mathbb{C}^{N\times 1}$ are narrowband baseband signal and zero mean additive white Gaussian noise (AWGN), respectively. $\boldsymbol{A} = [\boldsymbol{a}(\theta_1), \ldots, \boldsymbol{a}(\theta_M)] \in \mathbb{C}^{N\times M}$ represents the array manifold matrix, where $\boldsymbol{a}(\theta_m) = \left[1, e^{-j\frac{2\pi d}{\lambda}\sin(\theta_m)}, \ldots, e^{-j\frac{2\pi(N-1)d}{\lambda}\sin(\theta_m)}\right]^T \in \mathbb{C}^{N\times 1}$ is the steering vector and λ is the wavelength. $\boldsymbol{C} \in \mathbb{C}^{N\times N}$ is the MCM, which is regarded to be direction-independent.[20]

As reported in the work of Friedlander and Weiss,[20] the MC coefficient between any two equally spaced antenna elements is assumed to be the same. Moreover, it is also inversely related to the distance between the elements, and thus the MC coefficient will become approximately zero when any two elements are separated by several wavelengths. Therefore, in the case of a ULA $\boldsymbol{C}$ can be modeled as a banded symmetric Toeplitz matrix or a diagonal constant matrix, ie,

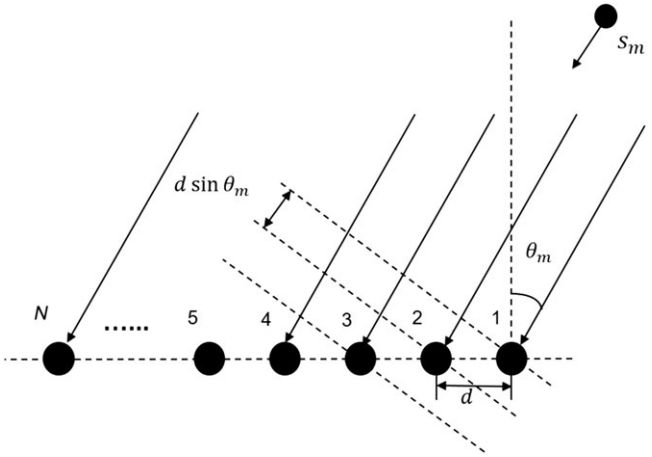

FIGURE 1 A uniform linear array system model

$\boldsymbol{C} = \text{Toeplitz}\{[\boldsymbol{c}^T, \boldsymbol{0}_{1\times(N-L)}]\}$. Here, $\boldsymbol{c} = [c_0, c_1, c_2, \ldots, c_{L-1}]^T \in \mathbb{C}^{L\times 1}$ is a complex vector consisting of L nonzero unique coupling coefficients. A symmetric Toeplitz matrix for any vector $\boldsymbol{v} = [v_0, v_1, \ldots, v_{L-1}]$ with length L is defined as

$$\text{Toeplitz}\{\boldsymbol{v}\} = \begin{bmatrix} v_0 & v_1 & \cdots & v_{L-1} \\ v_1 & v_2 & \cdots & v_{L-2} \\ \vdots & \vdots & \ddots & \vdots \\ v_{L-1} & v_{L-2} & \cdots & v_0 \end{bmatrix}. \tag{2}$$

We assume that the signals arriving at the antenna array are coherent such that all the received signals $\{s_m\}_{m=1}^M$ are attenuated and phase-delayed copies of the first signal, s_1, ie, $s_m(k) = b_m s_1(k)$, where b_m is a complex attenuation coefficient for the m^{th} signal. Assuming that the sources are uncorrelated with noise, the covariance matrix of $\boldsymbol{x}(k)$ is given by

$$\boldsymbol{R} = E\left[\boldsymbol{x}(k)\boldsymbol{x}^H(k)\right] = \boldsymbol{C}\boldsymbol{A}\boldsymbol{R}_s\boldsymbol{A}^H\boldsymbol{C}^H + \sigma_n^2\boldsymbol{I}_N \quad \in \mathbb{C}^{N\times N}, \tag{3}$$

where σ_n^2 is the noise variance, $E[\cdot]$ and $(\cdot)^H$ represent expectation and conjugate transpose operations, respectively. $\boldsymbol{R}_s = E\left[\boldsymbol{s}(k)\boldsymbol{s}^H(k)\right]$ is the signal covariance matrix, and $\boldsymbol{I}_N$ is an $N \times N$ identity matrix. When the signals are coherent, $\boldsymbol{R}_s$ becomes rank deficient. We can further express $\boldsymbol{R}_s$ as[17]

$$\boldsymbol{R}_s = E\left[\boldsymbol{s}(k)\boldsymbol{s}^H(k)\right] = \boldsymbol{b}\boldsymbol{b}^H E\left[s_1(k)s_1^H(k)\right], \tag{4}$$

where $\boldsymbol{b} = \left[b_1, b_2, \ldots, b_m\right]^T$ is an attenuation vector and $E\left[s_1(k)s_1^H(k)\right]$ is a constant corresponding to the variance of s_1. It can be seen from Equation (4) that the rank of $\boldsymbol{R}_s$ is one, or $r = 1$. This case, however, results in a matrix singularity, which ultimately leads to inaccurate estimates of DOA if conventional methods were to be used.

In order to transform the covariance matrix into a nonsingular matrix, a preprocessing method named FBSS technique is applied to the array outputs. For FBSS, we first group the array outputs into uniformly overlapping subarrays with the size z. Then, a spatially smoothed covariance matrix is obtained by averaging the covariance matrices of the subarray outputs.[16,17] Without MC effect, the p^{th} forward subarray, $\boldsymbol{x}_{f,p}(k)$, and p^{th} backward subarray, $\boldsymbol{x}_{b,p}(k)$, can be constructed as

$$\boldsymbol{x}_{f,p}(k) = \boldsymbol{A}_{fb}\boldsymbol{B}^{p-1}\boldsymbol{s}(k) + \boldsymbol{n}_{f,p}(k) \quad \in \mathbb{C}^{z\times 1} \tag{5}$$

$$\boldsymbol{x}_{b,p}(k) = \boldsymbol{A}_{fb}\boldsymbol{B}^{p-1}\boldsymbol{B}^{(z-1)^*}\boldsymbol{s}^*(k) + \boldsymbol{n}_{b,p}(k) \quad \in \mathbb{C}^{z\times 1}, \tag{6}$$

where

$$\boldsymbol{A}_{fb} = \left[\boldsymbol{a}_{fb}(\theta_1), \ldots, \boldsymbol{a}_{fb}(\theta_M)\right] \in \mathbb{C}^{z\times M} \tag{7}$$

$$\boldsymbol{a}_{fb}(\theta_m) = \left[1, e^{-j\frac{2\pi d}{\lambda}\sin(\theta_m)}, \ldots, e^{-j\frac{2\pi(z-1)d}{\lambda}\sin(\theta_m)}\right]^T \in \mathbb{C}^{z\times 1} \tag{8}$$

$$\boldsymbol{B} = \text{diag}\left\{e^{-j\frac{2\pi d}{\lambda}\sin(\theta_1)}, \ldots, e^{-j\frac{2\pi d}{\lambda}\sin(\theta_M)}\right\} \in \mathbb{C}^{M\times M}, \tag{9}$$

where $()^*$ denotes a complex conjugate. $\boldsymbol{n}_{f,p}(k) \in \mathbb{C}^{z\times 1}$ and $\boldsymbol{n}_{b,p}(k) \in \mathbb{C}^{z\times 1}$ are the AWGNs of the subarrays. The $(p-1)^{\text{th}}$ power of the diagonal matrix $\boldsymbol{B}$ acts as a forward-moving window, which helps to select the forward subarrays starting from the first antenna element. On the other hand, $\boldsymbol{B}^{p-1}\boldsymbol{B}^{(z-1)*}$ groups the backward subarrays starting from the last antenna

element. In the next section, for coherent signals case, we discuss a detailed approach that performs DOA estimation under unknown MC with low computational complexity and yet offering a similar performance as the conventional approaches with known MC.

3 | THE PROPOSED ALGORITHM

The proposed algorithm initially obtains the reduced-rank FBSS covariance matrix, which is then employed in the MV-based cost function of the autocalibration method to estimate the MC and DOAs iteratively. We firstly perform FBSS process on the array outputs to decorrelate the received signal. Then, the covariance matrix of the smoothed array output is reduced to a lower dimension by using JIO-based reduced-rank method. Finally, the reduced covariance matrix is applied to the MC autocalibration process to jointly estimate DOAs and MC coefficients. The complete procedure of the proposed algorithm is summarized in Algorithm 2 in Section 3.2.

3.1 | Spatial smoothing in the presence of mutual coupling

Here, we exploit the FBSS method,[17] which initially divides the original array output into $P = N - z + 1$ numbers of overlapping subarrays in both forward and backward directions at k^{th} snapshot in time domain. Mathematically, in the presence of MC, p^{th} forward subarray, $\boldsymbol{x}_{f,p}(k)$, and p^{th} backward subarray, $\boldsymbol{x}_{b,p}(k)$, can be written as

$$\boldsymbol{x}_{f,p}(k) = \boldsymbol{C}_{fb}\boldsymbol{A}_{fb}\boldsymbol{B}^{p-1}\boldsymbol{s}(k) + \boldsymbol{n}_{f,p}(k) \qquad \in \mathbb{C}^{z\times 1} \tag{10}$$

$$\boldsymbol{x}_{b,p}(k) = \boldsymbol{C}_{fb}\boldsymbol{A}_{fb}\boldsymbol{B}^{p-1}\boldsymbol{B}^{(z-1)^*}\boldsymbol{s}^*(k) + \boldsymbol{n}_{b,p}(k) \qquad \in \mathbb{C}^{z\times 1}, \tag{11}$$

where

$$\boldsymbol{C}_{fb} = \text{Toeplitz}\left\{\left[\boldsymbol{c}^T, \boldsymbol{0}_{1\times(z-L)}\right]\right\} \in \mathbb{C}^{z\times z}. \tag{12}$$

To determine the reduced-rank subarray output and its covariance matrix recursively, we first determine each subarray output in the JIO-based rank reduction process. Then, by using all P subarray outputs, the FBSS covariance matrix at k^{th} snapshot is calculated as

$$\boldsymbol{R}_{fb}(k) = \frac{1}{2P}\sum_{p=1}^{P}\left(\boldsymbol{R}_{f,p}(k) + \boldsymbol{R}_{b,p}(k)\right) \in \mathbb{C}^{z\times z}. \tag{13}$$

3.2 | JIO-FBSS–based reduced-rank DOA estimation with mutual coupling calibration

As a first step, the JIO-based reduced-rank method is modified in order to include the effect of MC. Using a rank reduction matrix $\boldsymbol{T}_{r,fb} \in \mathbb{C}^{z\times r}$ with reduced size r, the reduced-rank p^{th} forward and backward subarray outputs are obtained as

$$\bar{\boldsymbol{x}}_{f,p}(k) = \boldsymbol{T}_{r,fb}^H\boldsymbol{x}_{f,p}(k) \in \mathbb{C}^{r\times 1} \tag{14}$$

$$\bar{\boldsymbol{x}}_{b,p}(k) = \boldsymbol{T}_{r,fb}^H\boldsymbol{x}_{b,p}(k) \in \mathbb{C}^{r\times 1}. \tag{15}$$

Then, the new reduced-rank FBSS covariance matrix is obtained from Equation (13) by using reduced-rank covariance matrices, $\bar{\boldsymbol{R}}_{f,p}(k)$ and $\bar{\boldsymbol{R}}_{b,p}(k)$. Due to the symmetric structure of the ULA array, the matrix $\boldsymbol{C}_{fb}$ affecting the original steering vector can be transformed into a coupling vector $\boldsymbol{c}$ as

$$\boldsymbol{C}_{\boldsymbol{fb}}\boldsymbol{a}_{fb}(\theta) = \boldsymbol{T}\left[\boldsymbol{a}_{fb}(\theta)\right]\boldsymbol{c} \quad \in \mathbb{C}^{z\times 1}, \tag{16}$$

where $\boldsymbol{T}\left[\boldsymbol{a}_{fb}(\theta)\right] \in \mathbb{C}^{z\times L}$ is a ULA transformation matrix.[20] Consequently, $\bar{\boldsymbol{a}}_{fb}(\theta)$, the reduced-rank steering vector perturbed by MC becomes

$$\bar{\boldsymbol{a}}_{fb}(\theta) = \boldsymbol{T}_{r,fb}^H\boldsymbol{T}\left[\boldsymbol{a}_{fb}(\theta)\right]\boldsymbol{c} = \bar{\boldsymbol{T}}\left[\boldsymbol{a}_{fb}(\theta)\right]\boldsymbol{c} \in \mathbb{C}^{r\times 1}, \tag{17}$$

where $\bar{\boldsymbol{T}}\left[\boldsymbol{a}_{fb}(\theta)\right] = \boldsymbol{T}_{r,fb}^H\boldsymbol{T}\left[\boldsymbol{a}_{fb}(\theta)\right]$ is the reduced-rank $\boldsymbol{T}\left[\boldsymbol{a}_{fb}(\theta)\right]$. Given the new reduced rank variables, DOAs can be estimated by solving a modified MV-based reduced-rank optimization problem in the presence of MC[34] as

$$\begin{aligned} \hat{\theta}_m = \arg\min_{\theta} \quad & \bar{\boldsymbol{w}}_\theta^H\boldsymbol{T}_{r,fb}^H\boldsymbol{R}_{fb}\boldsymbol{T}_{r,fb}\bar{\boldsymbol{w}}_\theta \\ \text{subject to} \quad & \bar{\boldsymbol{w}}_\theta^H\boldsymbol{T}_{r,fb}^H\boldsymbol{T}\left[\boldsymbol{a}_{fb}(\theta)\right]\boldsymbol{c} = 1. \end{aligned} \tag{18}$$

Since the objective function, $\bar{\boldsymbol{w}}_\theta^H \boldsymbol{T}_{r,fb}^H \boldsymbol{R}_{fb} \boldsymbol{T}_{r,fb} \bar{\boldsymbol{w}}_\theta$, in Equation (18) is in quadratic form with linear constraint and the fact that $\boldsymbol{R}_{fb}$ is a symmetric positive semidefinite matrix, the function is convex.[36] Hence, the unknown variables $\bar{\boldsymbol{w}}_\theta(k)$ and $\boldsymbol{T}_{r,fb}(k)$ at each k^{th} snapshot are derived via the constrained least squares approach with Lagrange multiplier method as in the work of Wang et al,[14] resulting in Equations (22) and (23) of Algorithm 1 given as follows.

Algorithm 1 JIO-FBSS Algorithm with MC

for $\theta_i = -90 : \Delta : 90$ **do** ; ▷ Δ is a searching step size
  Initialize: $\boldsymbol{T}_{r,fb}(0) = \left[\boldsymbol{I}_{r\times r}^T \boldsymbol{0}_{r\times(z-r)}^T\right]^T$;
  $\hat{\boldsymbol{R}}_{fb}(0) = \delta \boldsymbol{I}_{z\times z}$; $\hat{\bar{\boldsymbol{R}}}_{fb}(0) = \delta \boldsymbol{I}_{r\times r}$; $\delta > 0$;
  for $k = 1 : 1 : K$ **do** ▷ Recursive with snapshot $k = 1, 2, \ldots, K$
    for $p = 1 : 1 : P$ **do** ▷ FBSS with subarray $p = 1, 2, \ldots, P$
      Calculate $\boldsymbol{x}_{f,p}(k)$ and $\boldsymbol{x}_{b,p}(k)$ using Equation (10) and Equation (11);
      Calculate $\bar{\boldsymbol{x}}_{f,p}(k)$ and $\bar{\boldsymbol{x}}_{b,p}(k)$ using Equation (14) and Equation (15);
      Calculate $\boldsymbol{R}_{f,p}(k) = \boldsymbol{x}_{f,p}(k)\boldsymbol{x}_{f,p}^H(k)$ and $\boldsymbol{R}_{b,p}(k) = \boldsymbol{x}_{b,p}(k)\boldsymbol{x}_{b,p}^H(k)$;
    end for
    Update $\hat{\bar{\boldsymbol{R}}}_{fb}(k)$ and $\boldsymbol{T}_{r,fb}(k)$ as follows:

$$\bar{\boldsymbol{T}}\left[\boldsymbol{a}_{fb}(\theta_i)\right] = \boldsymbol{T}_{r,fb}^H(k-1)\boldsymbol{T}\left[\boldsymbol{a}_{fb}(\theta_i)\right]; \tag{19}$$

$$\hat{\boldsymbol{R}}_{fb}(k) = \gamma \hat{\boldsymbol{R}}_{fb}(k-1) + \tfrac{1}{2P}\sum_{p=1}^{P}\left(\boldsymbol{R}_{f,p}(k) + \boldsymbol{R}_{b,p}(k)\right); \tag{20}$$

$$\hat{\bar{\boldsymbol{R}}}_{fb}(k) = \gamma \hat{\bar{\boldsymbol{R}}}_{fb}(k-1) + \tfrac{1}{2P}\sum_{p=1}^{P}\left(\bar{\boldsymbol{R}}_{f,p}(k) + \bar{\boldsymbol{R}}_{b,p}(k)\right); \tag{21}$$

$$\bar{\boldsymbol{w}}_\theta(k) = \frac{\hat{\bar{\boldsymbol{R}}}_{fb}^{-1}(k)\bar{\boldsymbol{T}}[\boldsymbol{a}_{fb}(\theta_i)]\boldsymbol{c}}{\boldsymbol{c}^H\bar{\boldsymbol{T}}^H[\boldsymbol{a}_{fb}(\theta_i)]\hat{\bar{\boldsymbol{R}}}_{fb}^{-1}(k)\bar{\boldsymbol{T}}[\boldsymbol{a}_{fb}(\theta_i)]\boldsymbol{c}}; \tag{22}$$

$$\boldsymbol{T}_{r,fb}(k) = \frac{\hat{\boldsymbol{R}}^{-1}(k)\boldsymbol{T}[\boldsymbol{a}_{fb}(\theta_i)]\boldsymbol{c}}{\boldsymbol{c}^H\boldsymbol{T}^H[\boldsymbol{a}_{fb}(\theta_i)]\hat{\bar{\boldsymbol{R}}}_{fb}^{-1}(k)\boldsymbol{T}[\boldsymbol{a}_{fb}(\theta_i)]\boldsymbol{c}}\frac{\bar{\boldsymbol{w}}_\theta^H(k)}{\|\bar{\boldsymbol{w}}_\theta(k)\|^2}; \tag{23}$$

  end for
  Calculate: $P_r(\theta_i)$ using Equation (24);
end for
return $P_r(\theta) = [P_r(\theta_1), P_r(\theta_2), \ldots, P_r(\theta_S)]$ ▷ S is length of θ

By recursively updating $\boldsymbol{T}_r(k)$ and $\bar{\boldsymbol{w}}_\theta(k)$ and substituting them into Equation (18), the reduced-rank Capon's power spectrum $P_r(\theta)$ is obtained as

$$P_r(\theta) = \left(\boldsymbol{c}^H\bar{\boldsymbol{T}}^H\left[\boldsymbol{a}_{fb}(\theta)\right]\hat{\bar{\boldsymbol{R}}}_{fb}^{-1}(K)\bar{\boldsymbol{T}}\left[\boldsymbol{a}_{fb}(\theta)\right]\boldsymbol{c}\right)^{-1}. \tag{24}$$

Using a forgetting constant γ, the estimate of $\bar{\boldsymbol{R}}_{fb}$ is recursively updated in each snapshot, and the estimated covariance matrix $\hat{\bar{\boldsymbol{R}}}_{fb}(K)$ is obtained after K snapshots.[37] The DOAs are then estimated by finding the peaks of the reduced-rank Capon's power spectrum $P_r(\boldsymbol{\theta})$. The overall algorithm is summarized in Algorithm 1.

In order to calibrate the coupling for the precise DOA estimation, the JIO-FBSS is combined with the autocalibration method. Compared to the autocalibration method,[23] which is based on MUSIC algorithm, the cost function to be minimized in the proposed method is based on MV criterion. This is because the algorithm of Wang et al[23] is valid only when the number of sources is less than the number of array sensors, or when $M \leq \left\lfloor \frac{(N-1)}{2} \right\rfloor$. However, in this study, N is reduced to r, where $r << N$, and therefore, the condition for the use of existing subspace-based calibration method is not fulfilled.

In JIO-FBSS, DOAs are estimated by maximizing the output power spectrum given in Equation (24). In this algorithm, DOAs and MC are iteratively updated by minimizing the sum of the inverse power spectrum, which corresponds to the true DOAs. Thus, the quadratic minimization problem based on Capon's power spectrum can be expressed as

$$\begin{aligned} \boldsymbol{c} = \arg\min_{\boldsymbol{c}} \quad & \sum_{m=1}^{M}\left[\left(\boldsymbol{c}^H\bar{\boldsymbol{T}}^H\left[\boldsymbol{a}_{fb}(\theta_m)\right]\hat{\bar{\boldsymbol{R}}}_{fb}^{-1}(K)\bar{\boldsymbol{T}}\left[\boldsymbol{a}_{fb}(\theta_m)\right]\boldsymbol{c}\right)^{-1}\right]^{-1} = \boldsymbol{c}^H\boldsymbol{G}(\theta)\boldsymbol{c} \\ \text{subject to} \quad & \|\boldsymbol{c}\| = 1, \end{aligned} \tag{25}$$

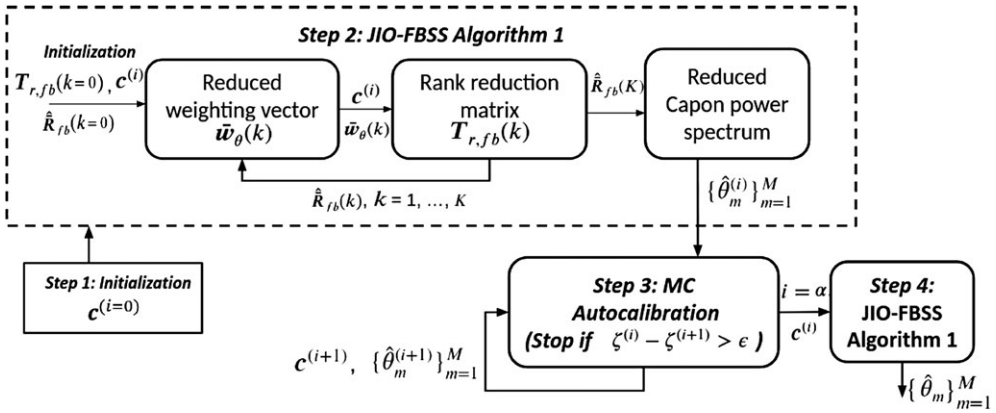

FIGURE 2 Summary of the proposed algorithm. FBSS, forward/backward spatial smoothing; JIO, joint iterative subspace optimization; MC, mutual coupling

where $\boldsymbol{G}(\theta) = \sum_{m=1}^{M} \bar{\boldsymbol{T}}^H \left[\boldsymbol{a}_{fb}(\theta_m)\right] \hat{\bar{\boldsymbol{R}}}_{fb}^{-1} \bar{\boldsymbol{T}} \left[\boldsymbol{a}_{fb}(\theta_m)\right]$. The solution to Equation (25) has already been discussed in the work of Wang et al[23] and is given as $\boldsymbol{c} = \boldsymbol{e}_{\min}\{\boldsymbol{G}(\theta)\}$, where $\boldsymbol{e}_{\min}\{\cdot\}$ denotes the eigenvector that corresponds to the smallest eigenvalue. After iteratively estimating $\boldsymbol{c}$ and $\{\hat{\theta}_m^{(i)}\}_{m=1}^{M}$ by the approach in Algorithm 2, the estimated $\boldsymbol{c}$ is determined when the convergence is reached. The final DOAs are estimated by using the updated $\boldsymbol{c}$ in Algorithm 1, which improves the DOA estimation accuracy. The summary of the proposed algorithm (Algorithm 2) is shown in Figure 2.

Algorithm 2 The proposed JIO-FBSS with MC autocalibration algorithm

Initialization:
$i = 0$, $\boldsymbol{c}^{(i)} = [1, \text{zeros}(1, L-1)]^T$;
Calculate $\hat{\bar{\boldsymbol{R}}}_{fb}^{-1}$, $\bar{\boldsymbol{T}}\left[\boldsymbol{a}_{fb}(\theta)\right]$ and $\{\hat{\theta}_m^{(i)}\}_{m=1}^{M}$ using Algorithm 1 with $\boldsymbol{c}^{(0)}$;
Calculate cost function $\zeta^{(i)} = \boldsymbol{c}^{(i)H}\boldsymbol{G}^{(i)}(\theta)\boldsymbol{c}^{(i)}$ with $\{\hat{\theta}_m^{(i)}\}_{m=1}^{M}$;
while true **do**
    Update $\boldsymbol{c}^{(i+1)} = \boldsymbol{e}_{\min}\{\boldsymbol{G}^{(i)}(\theta)\}$ with the previous $\{\hat{\theta}_m^{(i)}\}_{m=1}^{M}$;
    Normalize the $\boldsymbol{c}^{(i+1)}$ with the first element of the $\boldsymbol{c}^{(i+1)}$;
    Estimate new $\{\hat{\theta}_m^{(i+1)}\}_{m=1}^{M}$ with $\boldsymbol{c}^{(i+1)}$ in Equation (24);
    Calculate $\zeta^{(i+1)}$ and compare with $\zeta^{(i)}$;
    if $\zeta^{(i)} - \zeta^{(i+1)} > \epsilon$ **then** ▷ ϵ denotes the convergence threshold
        break **while** loop
    end if
    $i = i + 1$
end while ▷ number of iterations, α, is completed.
Estimate: new DOAs by using the final updated $\boldsymbol{c}^{(\alpha)}$ in the algorithm from Algorithm 1;

4 | SIMULATIONS

In this section, the performance of the proposed method is investigated and compared with those of FBSS-based algorithms with known coupling such as JIO-FBSS and Capon-FBSS, and MV-based autocalibration without rank reduction, or FBSS-calibration.[14,23] We consider a scenario where a ULA is composed of a relatively large number of $N = 50$ elements with $d = 0.5\lambda$. Moreover, we assume that only a small number of $K = 20$ snapshots are available. For an assumed $M = 4$ coherent signals impinging on the from $\boldsymbol{\theta} = [-55°, 40°, 45°, 60°]$, randomly chosen complex attenuation vector, $\mathbf{b}$, is set to $\boldsymbol{b} = [1, -0.3 - j0.7, 0.2 + j0.3, -0.1 + j0.6]$. Here, we consider a MC vector of $\boldsymbol{c} = [1, 0.6325 + j0.3946, 0.3514 + j0.2192]$ as given in the work of Qi et al,[21] $\Delta = 0.5°$ for a thorough scan, and $\gamma = 0.998$ as given in the study of Wang et al.[14] Following the work of Shan et al,[16] the subarray size for FBSS is chosen as $z = 41$, which results in $P = 10$ subarrays. The reduced rank is set to $r = 5$ since the rank that affects the resolution is between $r_{\min} = 3$ and $r_{\max} = 7$, which has been empirically proved.[14]

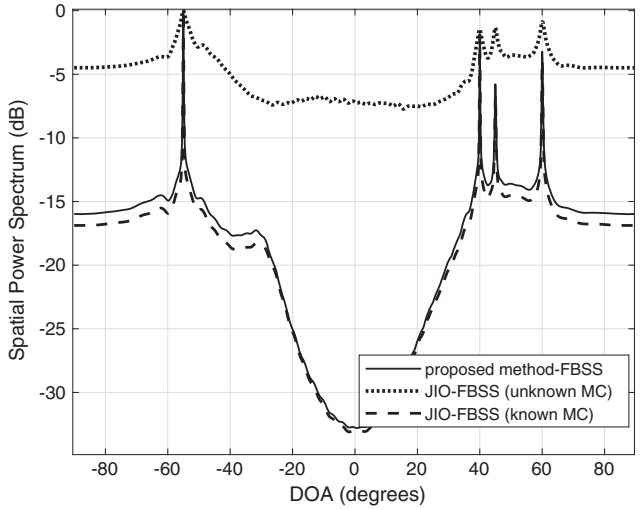

FIGURE 3 Comparison of spatial power spectra at SNR = 20 dB. DOA, direction of arrival; FBSS, forward/backward spatial smoothing; JIO, joint iterative subspace optimization; MC, mutual coupling; SNR, signal-to-noise ratio

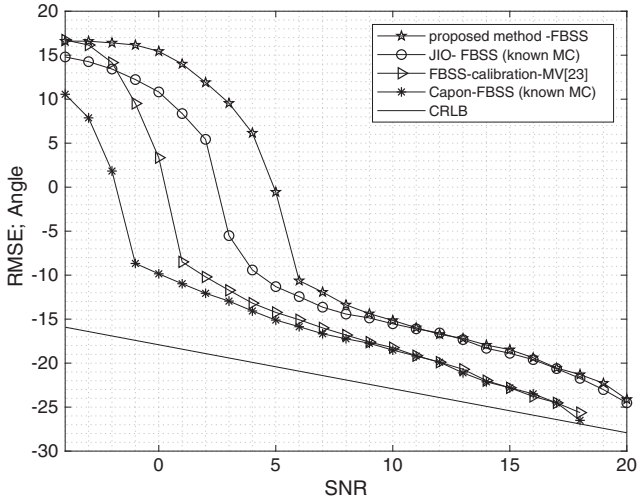

FIGURE 4 The root-mean-square errors (RMSEs) of direction of arrival (DOA) versus signal-to-noise ratio (SNR) at snapshot number = 20. CRLB, Cramer-Rao lower bound; FBSS, forward/backward spatial smoothing; JIO, joint iterative subspace optimization; MC, mutual coupling; MV, minimum variance

Simulations were initially run for the power spectra of the proposed approach at input signal-to-noise ratio (SNR) of 20 dB, and the results are compared with JIO-FBSS with no calibration and JIO-FBSS with known MC. The comparison for this case is given in Figure 3. It can be seen that the proposed method can estimate the true DOAs precisely with sharp peaks, similar to the JIO-FBSS with known MC. On the other hand, the spectrum peaks of JIO-FBSS with unknown MC are ambiguous even though FBSS helps to improve the DOA resolution. This shows that, at high SNR, the performance of the proposed method is as good as that of the JIO-FBSS algorithm with known coupling.

To get a better insight into the performance of the proposed approach, we also performed the comparisons in terms of RMSE of the DOA estimates. The RMSE is given as

$$\text{RMSE}\sqrt{\frac{1}{N_s M}\sum_{s=1}^{N_s}\sum_{m=1}^{M}\left|\hat{\theta}_m(s)-\theta_m(s)\right|^2}, \tag{26}$$

where N_s is the number of Monte Carlo simulations, and $\hat{\theta}_m(s)$ and $\theta_m(s)$ are estimated and true DOAs of m^{th} source at sth simulation, respectively. Figure 4 presents the RMSE performance for 1000 simulation runs ($N_s = 1000$). At low SNR levels, the RMSE values of the proposed method are larger than the other methods. As SNR increases, the RMSE curve

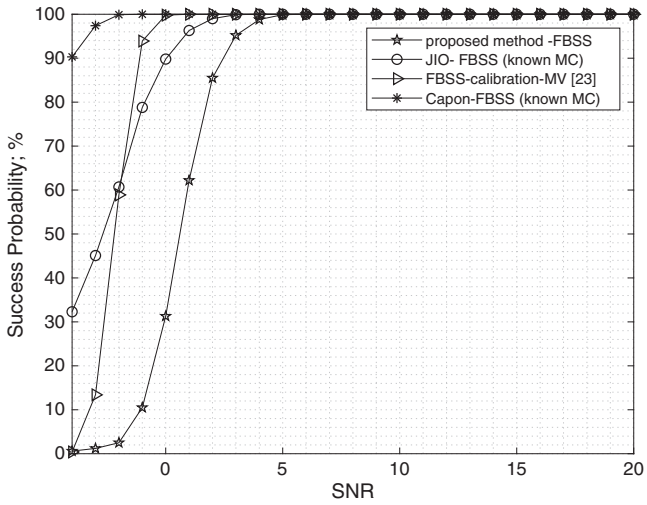

FIGURE 5 Probability of success versus signal-to-noise ratio (SNR) at snapshot number = 20. FBSS, forward/backward spatial smoothing; JIO, joint iterative subspace optimization; MC, mutual coupling; MV, minimum variance

of the proposed method becomes the same as JIO-FBSS with known MC and approximately follows the trends of both Capon-FBSS with known MC and FBSS-calibration method. In addition to the RMSE curves of the existing methods, the Cramer-Rao lower bound (CRLB) for noncoherent signals with known MC is also shown as a comparison. From the RMSE analysis, it can be stated that the proposed method works well for practical SNR levels. At very low SNR levels, the performance is lower due to the sensitivity of coupling estimation using reduced-rank covariance matrix, which, on the other hand, causes the complexity of the proposed method to be much lower than that of the others.

Next, we evaluate the probability of successful estimation versus SNR. Successful estimation is defined such that the average of the absolute estimation errors is within an estimation error threshold. The estimation error threshold is selected to be 2.5°, which is half a degree of the minimum DOA separation, so that when $|\hat{\theta}_m - \theta_m| < |\theta_m - \theta_{m+1}|/2$, the adjacent DOAs θ_m and θ_{m+1} are successfully separable.[14,38] As can be seen in Figure 5, Capon-FBSS algorithm with known MC is superior to the other given approaches. However, it requires a higher computational cost when compared with the proposed method and JIO-FBSS. Moreover, both Capon-FBSS and JIO-FBSS algorithms hold the same curve pattern when SNR increases since MC is known in both of the methods. On the other hand, the curves of the proposed method and FBSS with MC calibration follow the same trend due to their MC calibration. At low SNR regions, the proposed method has about 3 dB lower performance than the FBSS-calibration on average. However, this can be taken as a tradeoff between lower complexity and performance at lower SNR values. At high SNR values, the proposed method approaches a 100% success probability at 5 dB, followed by JIO-FBSS, FBSS-calibration, and Capon-FBSS, with approximately 2 dB difference. The proposed method achieves the 100% probability later than the other approaches because of its MC calibrating process.

In addition, the computational complexity of the proposed method is also compared and analyzed. Since FBSS-based algorithms are compared, we assume zero cost for FBSS step. While the method of Wang et al[23] has the complexity of $O\left(N^3 + \left(\frac{180}{\Delta}\right)N^2 + \alpha N^3\right)$, the proposed approach has $O\left(2\left[N^3 + \left(\frac{180}{\Delta}\right)r^3\right] + \left(\frac{180}{\Delta}\right)r^2 + \alpha r^3\right)$, where α denotes the number of iterations that achieves the convergence threshold described in Figure 2. The complexity of the algorithm of Wang et al[23] is due to the EVD of $\hat{\boldsymbol{R}}$ and $\boldsymbol{G}(\theta)$ and the grid search. As for the proposed method, $O\left(2\left[N^3 + \left(\frac{180}{\Delta}\right)r^3\right]\right)$ is due to the matrix inversion of the covariance matrix and the corresponding reduced-rank matrix in the rank-reduction process, which is repeated twice. The terms $O\left(\left(\frac{180}{\Delta}\right)r^2\right)$ and $O\left(\alpha r^3\right)$ are because of the grid search and EVD of reduced-rank $\boldsymbol{G}(\theta)$, respectively. For the simulation framework, since $r = 5$ and $N = 50$ were chosen, we have $r << N$, and thus the computational complexity of the proposed method is much lower than those of the conventional methods. For future 5G and beyond technologies, where large size of antenna array is deployed at BS, it is essential to implement low complexity–based signal processing algorithms since the computational complexity of the existing conventional algorithms becomes higher with the large number of antenna elements. Therefore, the proposed method, which exhibits a satisfactory performance for coherent signals at realistic SNR and with a lower complexity compared to the existing techniques, can be considered as one of the promising signal processing techniques in the future wireless communication systems.

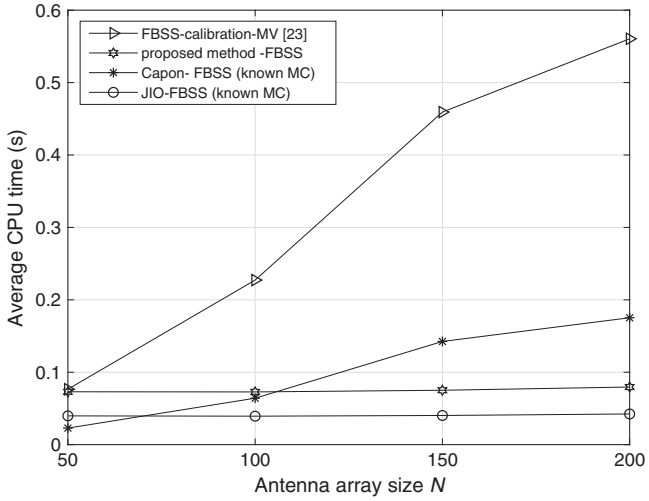

FIGURE 6 Average central processing unit (CPU) time versus antenna array size at SNR = 20 dB and K = 20. FBSS, forward/backward spatial smoothing; JIO, joint iterative subspace optimization; MC, mutual coupling; MV, minimum variance

Finally, the computational complexity is analyzed in terms of the average central processing unit (CPU) time in second (s). The simulations are performed for all the methods discussed previously by varying the antenna array size from $N = 50$ to $N = 200$ while fixing the number of snapshot at $K = 20$. This is because the effect of the antenna array size on the computational complexity is more dominant compared to that of the number of snapshot in these methods. SNR = 20 dB is assumed and the subarray size is fixed at $P = 10$ for FBSS process. Figure 6 shows the elapsed time of the DOA estimation for all methods, where the simulations are performed for 100 simulation runs on a computer with Linux Mint operating systems. The processor of the computer is Intel(R) Xeon(R) CPU E5-2650 v3 2.30 GHz x 10 and the memory is 188.8 GiB. As shown in Figure 6, the proposed method initially has a similar CPU elapsed time as the FBSS-calibration method without rank reduction at $N = 50$ because of the smaller size of the array resulting from FBSS process. However, as N becomes higher, the CPU time of the FBSS-calibration method increases rapidly. On the other hand, the CPU time of the proposed method does not change much, and it is less than FBSS-calibration method due to the fact that the reduced rank of the proposed method remains the same as the array size increases. Compared to the other methods with known MC, the proposed method has slightly larger CPU time because MC calibration process consumes some amount of time. It can also be observed that the proposed method and JIO-FBSS method have nearly constant CPU consumption time as N increases since both utilize a constant reduced rank.

5 | CONCLUSION

In this paper, we presented an extended version of reduced-rank DOA estimation for coherent signals impinging on an antenna array with unknown MC. The FBSS algorithm is initially performed for the JIO rank-reduction process, which gives the reduced covariance matrix. Then, the MC and the DOAs are iteratively updated by using the MV-based auto-calibration method. Finally, DOAs are estimated by JIO-FBSS rank-reduction method with the newly estimated coupling coefficients. Simulations show that the proposed algorithm can accurately perform DOA estimation of coherent signals with unknown MC especially at practical SNR levels. On the other hand, the performance of the proposed method at lower SNR levels is inferior to some existing studies due to less accurate MC estimation via reduced-rank covariance matrix. As opposed to the existing approaches, the proposed approach has a much lower computational complexity, which makes it more applicable to massive MIMO systems. In practice, MC changes with DOA of each incoming signal. Therefore, if one of the MC is known, higher DOA estimation accuracy can be achieved by employing the known MC as an initial coupling value in the calibration process. The proposed method can also be applied to the cases where there are groups of coherent signals arriving on the array from different directions.

ACKNOWLEDGMENTS

This study is supported by TÜBİTAK (project no 215E316) and TÜBİTAK 2215 BİDEB Scholarship Program. The authors also benefit from the fruitful discussion of Eurepean Union H2020 Cost Action CA15104 IRACON Meetings.

ORCID

Nann Win Moe Thet https://orcid.org/0000-0002-9193-1374

REFERENCES

1. Toşa F. Comparisons of beamforming techniques for 4G wireless communications systems. In: Proceedings of the 8th International Conference on Communications; 2010; Bucharest, Romania.
2. Shehata M, Hélard M, Crussière M, Rozé A, Langlais C. Angular based beamforming and power allocation framework in a multi-user millimeter-wave massive MIMO system. In: Proceedings of the 87th IEEE Vehicular Technology Conference (VTC Spring); 2018; Porto, Portugal.
3. Shafin R, Liu L. Multi-cell multi-user massive FD-MIMO: downlink precoding and throughput analysis. *IEEE Trans Wirel Commun*. 2019;18(1):487-502.
4. Lu L, Li GY, Swindlehurst AL, Ashikhmin A, Zhang R. An overview of massive MIMO: benefits and challenges. *IEEE J Sel Top Signal Process*. 2014;8(5):742-758.
5. Larsson EG, Edfors O, Tufvesson F, Marzetta TL. Massive MIMO for next generation wireless systems. *IEEE Commun Mag*. 2014;52(2):186-195.
6. Artiga X, Devillers B, Perruisseau-Carrier J. Mutual coupling effects in multi-user massive MIMO base stations. In: Proceedings of the 2012 IEEE International Symposium on Antennas and Propagation; 2012; Chicago, IL.
7. Ozdemir MK, Arslan H, Arvas E. Mutual coupling effect in multiantenna wireless communication systems. In: Proceedings of the IEEE Global Telecommunications Conference (GLOBECOM); 2003; San Francisco, CA.
8. Ozdemir MK, Arvas E, Arslan H. Dynamics of spatial correlation and implications on MIMO systems. *IEEE Commun Mag*. 2004;42(6):S14-S19.
9. Capon J. High-resolution frequency-wavenumber spectrum analysis. *Proc IEEE*. 1969;57(8):1408-1418.
10. Paulraj A, Roy R, Kailath T. Estimation of signal parameters via rotational invariance techniques-ESPRIT. In: Proceedings of the 19th IEEE Asilomar Conference on Circuits, Systems and Computers; 1985; Pacific Grove, CA.
11. Roy R, Kailath T. ESPRIT-estimation of signal parameters via rotational invariance techniques. *IEEE Trans Acoust Speech Signal Process*. 1989;37(7):984-995.
12. Schmidt R. Multiple emitter location and signal parameter estimation. *IEEE Trans Antennas Propag*. 1986;34(3):276-280.
13. Poormohammad S, Farzaneh F. Precision of direction of arrival (DOA) estimation using novel three dimensional array geometries. *AEU Int J Electron Commun*. 2017;75:35-45.
14. Wang L, de Lamare RC, Haardt M. Direction finding algorithms based on joint iterative subspace optimization. *IEEE Trans Aerosp Electron Syst*. 2014;50(4):2541-2553.
15. Qiu L, Cai Y, de Lamare RC, Zhao M. Reduced-rank DOA estimation algorithms based on alternating low-rank decomposition. *IEEE Signal Process Lett*. 2016;23(5):565-569.
16. Shan T-J, Wax M, Kailath T. On spatial smoothing for direction-of-arrival estimation of coherent signals. *IEEE Trans Acoust Speech Signal Process*. 1985;33(4):806-811.
17. Pillai SU, Kwon BH. Forward/backward spatial smoothing techniques for coherent signal identification. *IEEE Trans Acoust Speech Signal Process*. 1989;37(1):8-15.
18. Hari KVS, Ramakrishnan BV. Performance analysis of a modified spatial smoothing technique for direction estimation. *Signal Processing*. 1999;79(1):73-85.
19. Gupta I, Ksienski A. Effect of mutual coupling on the performance of adaptive arrays. *IEEE Trans Antennas Propag*. 1983;31(5):785-791.
20. Friedlander B, Weiss AJ. Direction finding in the presence of mutual coupling. *IEEE Trans Antennas Propag*. 1991;39(3):273-284.
21. Qi C, Wang Y, Zhang Y, Chen H. DOA estimation and self-calibration algorithm for uniform circular array. *IET Electronics Letters*. 2005;41(20):1092-1094.
22. Sellone F, Serra A. A novel online mutual coupling compensation algorithm for uniform and linear arrays. *IEEE Trans Signal Process*. 2007;55(2):560-573.
23. Wang M, Ma X, Yan S, Hao C. An autocalibration algorithm for uniform circular array with unknown mutual coupling. *IEEE Antennas Wirel Propag Lett*. 2016;15:12-15.
24. Jiang G, Dong Y, Mao X, Liu Y. Improved 2D direction of arrival estimation with a small number of elements in UCA in the presence of mutual coupling. *AEU Int J Electron Commun*. 2017;71:131-138.
25. Wu H, Hou C, Chen H, Liu W, Wang Q. Direction finding and mutual coupling estimation for uniform rectangular arrays. *Elsevier Signal Processing*. 2015;117:61-68.
26. Shaghaghi M, Vorobyov SA. Subspace leakage analysis and improved DOA estimation with small sample size. *IEEE Trans Signal Process*. 2015;63(12):3251-3265.
27. Zhou H, Hu G, Shi J, Feng Z. Orthogonal projection method for DOA estimation in low-altitude environment based on signal subspace. *AEU Int J Electron Commun*. 2018;83:317-321.
28. Dai J, Ye Z. Spatial smoothing for direction of arrival estimation of coherent signals in the presence of unknown mutual coupling. *IET Signal Process*. 2011;5(4):418-425.

29. Liao B, Chan SC. DOA estimation of coherent signals for uniform linear arrays with mutual coupling. In: Proceedings of the IEEE International Symposium of Circuits and Systems (ISCAS); 2011; Rio de Janeiro, Brazil.
30. Shi H, Li Z, Liu D, Chen H. Efficient method of two-dimensional DOA estimation for coherent signals. *EURASIP J Wirel Commun Netw*. 2017;2017(1):53.
31. Shi J, Hu G, Sun F, Zong B, Wang X. Improved spatial differencing scheme for 2-D DOA estimation of coherent signals with uniform rectangular arrays. *Sensors*. 2017;17(9):1956.
32. Qi C, Chen Z, Wang Y, Zhang Y. DOA estimation for coherent sources in unknown nonuniform noise fields. *IEEE Trans Aerosp Electron Syst*. 2007;43(3):1195-1204.
33. Kachroo A. *Joint Estimation of Direction of Arrival With Unknown Mutual Coupling in Massive MIMO Networks and LTE Radio Resource Block Allocation Optimization in Maritime Channels* [master's thesis]. Istanbul, Turkey: Electronic and Computer Engineering, Istanbul Şehir Üniversitesi; 2017.
34. Thet NWM, Ozdemir MK, Kachroo A. Reduced-rank joint estimation of DOA with mutual coupling. In: Proceedings of the 26th Signal Processing and Communications Applications Conference (SIU); 2018; Izmir, Turkey.
35. Elbir AM. Direction finding in the presence of direction-dependent mutual coupling. *IEEE Antennas Wirel Propag Lett*. 2017;16:1541-1544.
36. Boyd S, Vandenberghe L. *Convex Optimization*. Cambridge, UK: Cambridge University Press; 2004.
37. Haykin S. *Adaptive Filter Theory*. London, UK: Pearson Higher Education; 2013.
38. Stoica P, Gershman AB. Maximum-likelihood DOA estimation by data-supported grid search. *IEEE Signal Process Lett*. 1999;6(10):273-275.

How to cite this article: Thet NWM, Kachroo A, Ozdemir MK. Extended reduced-rank joint estimation of direction of arrival with mutual coupling for coherent signals. *Trans Emerging Tel Tech*. 2019;e3620. https://doi.org/10.1002/ett.3620